

Tyrosine phosphorylated Par3 regulates epithelial tight junction assembly promoted by EGFR signaling

Yiguo Wang^{1,2}, Dan Du^{1,2}, Longhou Fang^{1,2}, Guang Yang^{1,2}, Chenyi Zhang¹, Rong Zeng¹, Axel Ullrich³, Friedrich Lottspeich⁴ and Zhengjun Chen^{1,5,*}

¹Key Laboratory of Proteomics and Laboratory of Molecular Cell Biology, Institute of Biochemistry and Cell Biology, Shanghai Institutes for Biological Sciences, Chinese Academy of Sciences, Shanghai, China, ²Graduate School of the Chinese Academy of Sciences, Beijing, China, ³Department of Molecular Biology, Max-Planck-Institute of Biochemistry, Martinsried, Germany, ⁴Protein Analytik, Max-Planck-Institute of Biochemistry, Martinsried, Germany and ⁵SHARF Laboratory, Shanghai, China

The conserved polarity complex, comprising the partitioning-defective (Par) proteins Par3 and Par6, and the atypical protein kinase C, functions in various cell-polarization events and asymmetric cell divisions. However, little is known about whether and how external stimuli-induced signals may regulate Par3 function in epithelial cell polarity. Here, we found that Par3 was tyrosine phosphorylated through phosphoproteomic profiling of pervanadate-induced phosphotyrosine proteins. We also demonstrated that the tyrosine phosphorylation event induced by multiple growth factors including epidermal growth factor (EGF) was dependent on activation of Src family kinase (SFK) members c-Src and c-Yes. The tyrosine residue Y1127 (Y1127) of Par3 was identified as the major EGF-induced phosphorylation site. Moreover, we found that Y1127 phosphorylation reduced the association of Par3 with LIM kinase 2 (LIMK2), thus enabling LIMK2 to regulate cofilin phosphorylation dynamics. Substitution of Y1127 for phenylalanine impaired the EGF-induced Par3 and LIMK2 dissociation and delayed epithelial tight junction (TJ) assembly considerably. Collectively, these data suggest a novel, phosphotyrosine-dependent fine-tuning mechanism of Par3 in epithelial TJ assembly controlled by the EGF receptor-SFK signaling pathway.

The EMBO Journal (2006) 25, 5058–5070. doi:10.1038/sj.emboj.7601384; Published online 19 October 2006

Subject Categories: cell & tissue architecture; signal transduction

Keywords: EGFR signaling; LIMK2; Par3; phosphotyrosine; tight junction

Introduction

Cell polarity is vital for the development of multicellular organisms and for the proper functions of epithelial cells in different organs, the dysfunction of which is closely related with many diseases, including cancer (Sawada *et al*, 2003). The mammalian homologs of the *Caenorhabditis elegans* partitioning-defective (Par) proteins are necessary for establishing cell polarity. In mammalian epithelial cells, the Par3/Par6/aPKC polarity complex is localized to the tight junctions (TJs), where it regulates TJ formation and positioning with respect to basolateral and apical membrane regions (Ohno, 2001; Matter and Balda, 2003; Macara, 2004). To date, various proteins, including Cdc42 (Joberty *et al*, 2000; Lin *et al*, 2000), T-lymphoma invasion and metastasis 1 (Tiam1) (Chen and Macara, 2005; Nishimura *et al*, 2005), LIM kinase 2 (Chen and Macara, 2006), 14-3-3 ζ (Hurd *et al*, 2003a), lethal giant larva (lgl) (Plant *et al*, 2003), and proteins associated with Lin Seven 1 (PALS1) (Hurd *et al*, 2003b), were found to interact with the Par protein complex, and positively or negatively regulate the epithelial TJ assembly through the 'calcium switch' model. Overexpressed Par3 could promote TJ formation, whereas the knock down of Par3 leads to a dramatic delay of TJ assembly (Hirose *et al*, 2002; Chen and Macara, 2005, 2006). However, it is unclear how these polarity complexes signal and stimulate polarization in response to external stimuli (Matter and Balda, 2003; Matter *et al*, 2005).

Growth factors, cytokines, and G protein-coupled receptor (GPCR) signaling pathways are reportedly involved in various key cellular processes, such as cell division, differentiation, survival, and cell polarity, including epithelial TJ assembly and disassembly (Sawada *et al*, 2003; Schwabe *et al*, 2005). For instance, the hepatocyte growth factor (HGF) induces scattering, migration, tubulogenesis, and pseudostratified layer morphogenesis of cultured Madin-Darby Canine Kidney (MDCK) epithelial cells (Pollack *et al*, 2004). The platelet-derived growth factor (PDGF) mediates TJ disassembly, and increases the permeability of MDCK cells (Harhaj *et al*, 2002). The orphan GPCR Moody, the G protein α subunits Gi and Go, and their regulator Loco mediate a complicated and common pathway that regulates the formation of the septate junctions (SJs) of the blood-brain barrier in *Drosophila* (Schwabe *et al*, 2005). Through systematic analysis, Par6 was found to interact with the transforming growth factor β (TGF β) receptor, which is required for serine phosphorylation of Par6. The phosphorylated Par6 recruits E3 ubiquitin ligase Smurf1 and results in the degradation of RhoA, and controls the transition of cells from epithelial to mesenchymal phenotypes (Ozdamar *et al*, 2005). EGF signaling reportedly controls TJ formation through inducing claudin expression by activating the MAPK pathway (Singh and Harris, 2004), and regulating the translocation of TJ proteins from the cytoplasm to cell-cell contact (Yoshida *et al*, 2005).

*Corresponding author. Institute of Biochemistry and Cell Biology, Shanghai Institutes for Biological Sciences, Chinese Academy of Sciences, 320 Yue Yang Road, Shanghai 200031, China.
Tel.: 86 21 54921081; Fax: 86 21 54921081; E-mail: zjchen@sibs.ac.cn

Received: 5 May 2006; accepted: 12 September 2006; published online: 19 October 2006

Taken together, there are likely multiple complexes and steps involved in TJ assembly and disassembly that are tightly regulated by different signaling pathways (Gonzalez-Mariscal *et al*, 2003). However, the nature of the signaling events is not well defined. Therefore, it is intriguing to explore the signaling regulatory mechanism of TJ complexes involved in TJ assembly and cell polarity formation.

There is emerging evidence that protein phosphorylation is a key mechanism by which polarity proteins are regulated. For instance, aPKC has been demonstrated to phosphorylate Par3 at serines 827 and 114, which may regulate the interaction of Par3–aPKC and -14-3-3 ζ , respectively (Hirose *et al*, 2002; Hurd *et al*, 2003a). In addition, aPKC hyper-phosphorylates Igl (Plant *et al*, 2003), another polarity protein implicated in targeted vesicle trafficking. Protein phosphatase 2A appears able to affect aPKC, as well as the phosphorylation of individual TJ components, and can therefore inhibit aPKC function and trigger junction disassembly (Nunbhakdi-Craig *et al*, 2002). EMK1 and LKB1, serine/threonine kinases related to the *C. elegans* Par1 and Par4 gene products, respectively, are also emerging as key regulators of cell polarity in lower and higher eukaryotes (Spicer and Ashworth, 2004; Vinot *et al*, 2005). Recently, several lines of evidence indicate that the Src family kinases (SFKs) phosphorylate TJ proteins, including ZO-1, ZO-2, and occludin, leading to positive and negative regulation of TJ formation (Yap *et al*, 1997; Tsukamoto and Nigam, 1999; Chen *et al*, 2002). However, the regulatory mechanism of the SFKs in TJ formation is not fully understood.

In this study, we conducted a proteomic analysis of pervanadate-induced phosphotyrosine proteins and found that a tyrosine residue (Y1127) of Par3 is phosphorylated. We further demonstrated that the EGF signaling pathway phosphorylates this tyrosine via c-Src and c-Yes, which provide the upstream signals for Par3 activation. Par3 functions as a novel component of the EGF-signaling pathway to regulate EGF-promoted epithelial TJ formation through a novel, tyrosine phosphorylation-dependent mechanism.

Results

Tyrosine phosphorylation of Par3 induced by EGF

To search for novel phosphotyrosine proteins, we analyzed pervanadate-induced phosphotyrosine proteins (POV, a protein tyrosine phosphatase-specific inhibitor) using subcellular fractionation, affinity purification, and tandem mass spectrometry (Supplementary Figure S1 and Supplementary Table S1). We identified 124 phosphotyrosine sites derived from 130 proteins (Supplementary Table S1), over 50% of which are not documented in Human Protein Reference Database (HPRD), Phosphosite, and Swiss-prot database. Among the phosphotyrosine proteins identified, Par3, a cell polarity protein, is of special interest to us. Par3 usually forms a complex with Par6 and aPKC, and plays an important role in establishing and maintaining cellular polarity (Ohno, 2001; Macara, 2004). To investigate the signaling pathway(s) that may control Par3 tyrosine phosphorylation, we transiently cotransfected 293T cells with Par3 and various growth factor receptors, including EGFR, PDGFR, fibroblast growth factor receptor (FGFR), nerve growth factor receptor (NGFR), and insulin receptor (IR). Par3 phosphorylation was analyzed by immunoblots using anti-phosphotyrosine antibodies (4G10).

As shown in Figure 1A, tyrosine phosphorylation of Par3 was clearly increased when EGFR, PDGFR, FGFR, NGFR, and IR were overexpressed in 293T cells, indicating that Par3 may be involved in multiple growth factor receptor signaling pathways. The transfection efficacy of the receptor tyrosine kinases (RTKs) was indicated by assaying for cellular total tyrosine phosphorylation using Western blots (Supplementary Figure S2). EGFR displayed the strongest effect on Par3 tyrosine phosphorylation, compared to the other RTKs (Figure 1A, lane 2), suggesting that EGFR-initiated signaling may dominantly regulate the tyrosine phosphorylation of Par3 in these cells. Thus, EGFR was investigated further to determine its role in regulating Par3 phosphorylation.

To investigate EGF-induced Par3 phosphorylation in native cells, we generated a specific antibody against the PDZ2-3 domains of Par3 (anti-PDZ 2-3). Par3 has three splice forms, known as 180K, 150K, and 100K (Figure 1B) (Lin *et al*, 2000). Western blot analysis with 4G10 revealed that EGF stimulation induced the phosphorylation of the Par3 180K form exclusively, and not the 150K and 100K forms in 293T and MDCK cells (Figure 1C, upper panel). The anti-PDZ 2-3 antibody recognized all three splice forms of Par3 in the 293T and MDCK cells (Figure 1C, low panel). We obtained the same results in 293T cell overexpression system, in which the three Par3 forms were transfected into 293T cells in the presence or absence of EGF (Figure 1D). According to structural differences among the three Par3 forms (Figure 1B), we inferred that the EGF-induced phosphotyrosine site(s) are located in the C-terminus of the Par3 180K form. Thus, our subsequent experiments focused on Par3 180K form.

Requirement of c-Src and/or c-Yes for tyrosine phosphorylation of Par3

Next, we were interested in identifying the kinase responsible for the EGF-induced tyrosine phosphorylation of Par3. To address this issue, a specific antibody to the C-terminus of Par3 (anti-Par3 LCT) was generated, which exhibited no cross-reaction with the other two splice forms of Par3 (data not shown). Immunoprecipitation experiments with the anti-LCT or anti-EGFR antibodies did not detect any interaction between EGFR and Par3 (data not shown), indicating that EGFR may indirectly mediate Par3 phosphorylation. Because the SFKs are the key downstream kinases responsible for transducing and amplifying the EGFR-initiated signals (Bromann *et al*, 2004), we then asked whether the SFKs phosphorylate Par3. To test this, we used PP2, a common SFKs inhibitor. The 293T and MDCK cells were treated with or without PP2 before EGF stimulation. Without PP2 treatment, Par3 underwent tyrosine phosphorylation in response to EGF stimulation in both cell lines (Figure 2A and B, lanes 1 and 2). In contrast, when the cells were treated with PP2, this phosphorylation was abolished (Figure 2A and B, lanes 3 and 4). In MDCK cells, PP2 also inhibited the basal level of Par3 phosphorylation. These results suggested that the activation of the SFKs might be required for the EGF-induced tyrosine phosphorylation of Par3. To determine which member of the SFK family mediates Par3 phosphorylation, we employed an RNA interference (RNAi) approach. There are nine identified and described SFK family members thus far (Bromann *et al*, 2004). However, c-Src, c-Yes, and Fyn are dominantly expressed in MDCK cells and a variety of other cell types, whereas the other members are expressed primar-

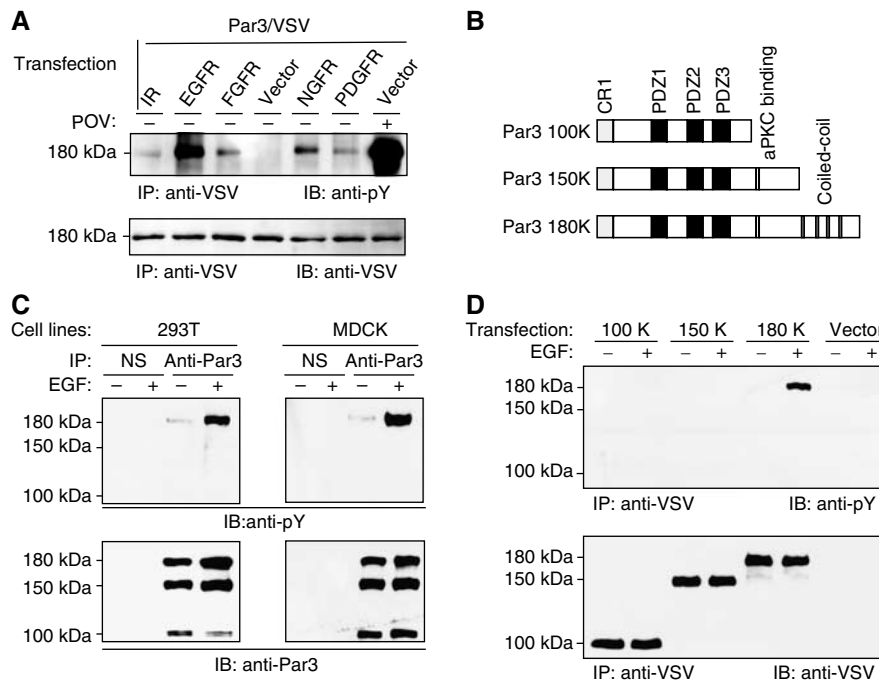


Figure 1 EGF-induced tyrosine phosphorylation of Par3 180K form. (A) Cotransfection of VSV-tagged Par3 with various growth factor receptors in 293T cells. The VSV-tagged Par3 plasmids were cotransfected with EGFR, PDGFR, NGFR, insulin receptor (IR), FGFR, or empty vectors into 293T cells, treated with or without pervanadate for 10 min. The total cell lysates were immunoprecipitated and immunoblotted as indicated. (B) Schematic representations of 100, 150, and 180kDa splice forms of Par3. The conserved region (CR1), the three PDZ domains, and the aPKC-binding region are shown. The coiled-coil domains were predicted by Pfam (<http://www.sanger.ac.uk/cgi-bin/Pfam>). (C) Total cell lysates from 293T and MDCK cells stimulated (not for controls) with EGF, immunoprecipitated with rabbit anti-Par3 (PDZ 2-3) or control nonimmune serum (NS), and immunoblotted with anti-pY or anti-Par3 (PDZ 2-3). (D) Three VSV-tagged forms of Par3, 180K, 150K, and 100K, or empty vectors were transfected into 293T cells stimulated (not for controls) with EGF. Total cell lysates were immunoprecipitated and immunoblotted as indicated.

ily in hematopoietic cells (Sargiacomo *et al*, 1993; Park and Cartwright, 1995). We first prepared small interfering RNAs (siRNA), which target canine c-Src, c-Yes, and Fyn (Supplementary Table S2), and applied them to MDCK cells to suppress the expression of endogenous c-Src, c-Yes, and Fyn, respectively. As shown in Figure 2C, each siRNA for the three kinases sufficiently and specifically suppresses the endogenous expression of corresponding members of SFKs in MDCK cells. No cross-suppression among the three kinases was observed (data not shown). A combination of the two-selected siRNAs produced a more efficient knockdown of the targeted genes (Figure 2C, last lane), and this strategy was used in our subsequent experiments. As shown in Figure 2D, EGF-induced tyrosine phosphorylation of Par3 was remarkably reduced in cells transfected with the siRNAs for c-Src or c-Yes, but not with Fyn siRNAs. More interestingly, a double knockdown of Src and Yes almost completely abolished the tyrosine phosphorylation of Par3 (Figure 2D, last lane). These results suggest strongly that both c-Src and c-Yes, but not Fyn are required for EGF-induced phosphorylation of Par3 in MDCK cells.

Identification of Par3 Y1127 residue as the major EGF-induced phosphotyrosine site

As the C-terminus of Par3 (LCT) contains 14 potential tyrosine phosphorylation sites (Supplementary Figure S3A), we next ascertained the tyrosine residue that is targeted by SFKs in response to EGF stimulation. According to Scansite prediction, five of these sites, Y1080, Y1098, Y1127, Y1259, and

Y1313, were well matched with SFK target motifs (Supplementary Figure S3A). The Y1127 residue was identified as a novel phosphorylation site by the LC-MS/MS (Supplementary Table S1). However, the identity of the Par3 C-terminal tyrosine residues that are phosphorylated by the SFK family was still unclear. To identify these sites, we performed *in vitro* phosphorylation of Par3 LCT using a kinase assay and commercial purified c-Src kinase. As shown in Figure 3A, the Par3 LCT-GST fusion protein, but not the GST protein was phosphorylated when c-Src kinase was included in the incubation reaction (Figure 3A, right), indicating that Par3 LCT may be a direct substrate for SFKs. The phosphorylated fusion protein was further sequenced by MS analysis. From the sequencing analysis, we identified 23 polypeptides that spanned nearly 80% of the Par3 C-terminus (Supplementary Table S3), including 11 of the 14 C-terminus tyrosine residues. As shown in Figure 3B and Supplementary Figure S3B and S3C, three tyrosine residues, Y1127, Y1177, and Y1321, were identified as phosphotyrosine sites by the MS, respectively. Additionally, the alignment of these sites shows the conservation of the Y1127 phosphorylation motif, a potential C-terminus Src kinase (Csk)-binding motif (Songyang *et al*, 1994), from chicken to human (Figure 3C), indicating the functional importance of this site.

To investigate which tyrosine of these three actually incurs phosphorylation *in vivo* by EGF signaling, we introduced single point mutations Y1127F, Y1177F, and Y1321F of Par3, and transfected these constructs into MDCK cells. The wild-type Par3 underwent tyrosine phosphorylation in response to

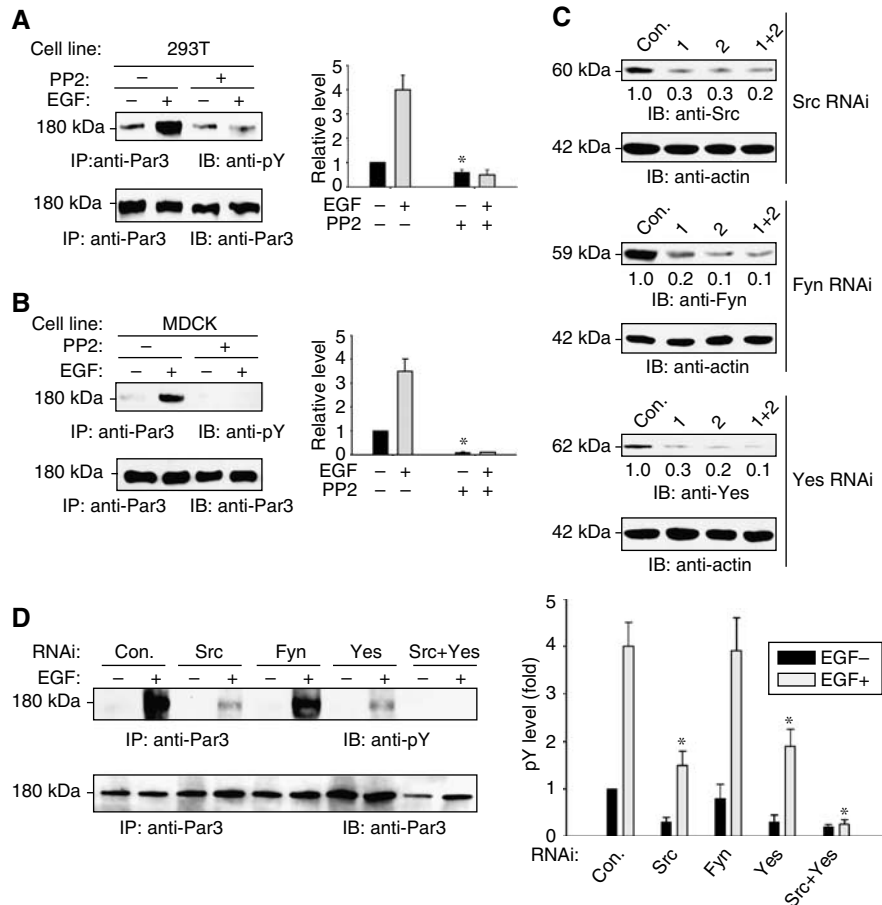


Figure 2 c-Src and c-Yes are required for EGF-induced tyrosine phosphorylation of Par3. 293T (**A**) and MDCK (**B**) cells were stimulated with or without EGF for 10 min after PP2 treatment for 30 min, respectively. The total cell lysates were immunoprecipitated with anti-Par3 (LCT), and immunoblotted with anti-pY or anti-Par3 (LCT). The quantification of the immunoblots is shown in the near right panel. Each value represents the mean \pm s.e.m. of triplicate experiments. Asterisks denote significant differences from cells without PP2 ($P < 0.05$), as determined with a Student's *t*-test. (**C**) Src family kinase knockdown efficiencies. MDCK cells were transiently transfected with empty vector (control) or constructs targeting different sequences of canine SFKs mRNA. Equal amounts of total proteins were analyzed with immunoblotting as indicated. The relative levels are shown. (**D**) The knockdown of c-Src and c-Yes decreases the phosphotyrosine levels of Par3. MDCK cells were transiently transfected with empty vector (control) or two constructs targeting canine SFKs mRNA sequences, immunoprecipitated with anti-Par3 (LCT), and immunoblotted as indicated. The quantification of the immunoblots is shown in the right panel. Each value represents the mean \pm s.e.m. of triplicate experiments. * $P < 0.05$ versus control.

EGF stimulation (Figure 3D, lanes 3 and 4, and right panel columns 3 and 4). Tyrosine phosphorylation of Y1127F was notably reduced compared to the wild type (lanes 5 and 6, and columns 5 and 6), whereas that of Y1177F and Y1321F manifested no significant changes. Taken together, our results suggest that Par3 Y1127 is the major phosphotyrosine site *in vivo* in response to EGF stimulation.

Necessity of c-Src and c-Yes for EGF-induced epithelial TJ assembly

A bidirectional synergistic interaction between EGFR and Src promotes distinct cellular actions, such as proliferation and cell transformation (Ishizawa and Parsons, 2004). However, it is unclear whether SFK is required for EGFR-evoked TJ assembly in epithelial cells, although SFKs and EGFR reportedly modulate TJ formation through different mechanisms (Van Itallie *et al*, 1995; Chen *et al*, 2002; Singh and Harris, 2004; Yoshida *et al*, 2005; Basuroy *et al*, 2006). To address this issue, we examined the effect of PP2 on the immunolocalization of Par3 and ZO-1 in confluent MDCK cells in the

presence of EGF or a vehicle control. Control cells were unable to form the complete TJ ring structure, even after 24 h of stimulation with control vehicles (Figure 4A, panels 1 and 2, and B, columns 1–3). In contrast to the control cells, approximately 95% of MDCK cells completed the TJ structure with both Par3 and ZO-1 labeling after 12 h of EGF treatment (Figure 4A, panel 3, top and B, column 5), and were stably maintained up to 24 h (Figure 4A, panel 3, bottom and B, column 6). However, when the cells were treated with PP2 before EGF stimulation, the complete TJ ring only reached about 50 and 80% after 12 and 24 h incubation with EGF, respectively (Figure 4A, panel 4 and B, columns 8 and 9).

As transepithelial electrical resistance (TER) reflects paracellular permeability regulated by the TJ, the *de novo* formation of TJ can be followed through the development of TER (Hirose *et al*, 2002; Chen and Macara, 2005). As shown in Figure 4C, the TER developed rapidly, peaking to $5152 \pm 110 \Omega \text{cm}^2$ at 12 h in the cells stimulated with EGF. However, the TER was unable to develop in the cells without EGF stimulation. Although the TER developed in the cells

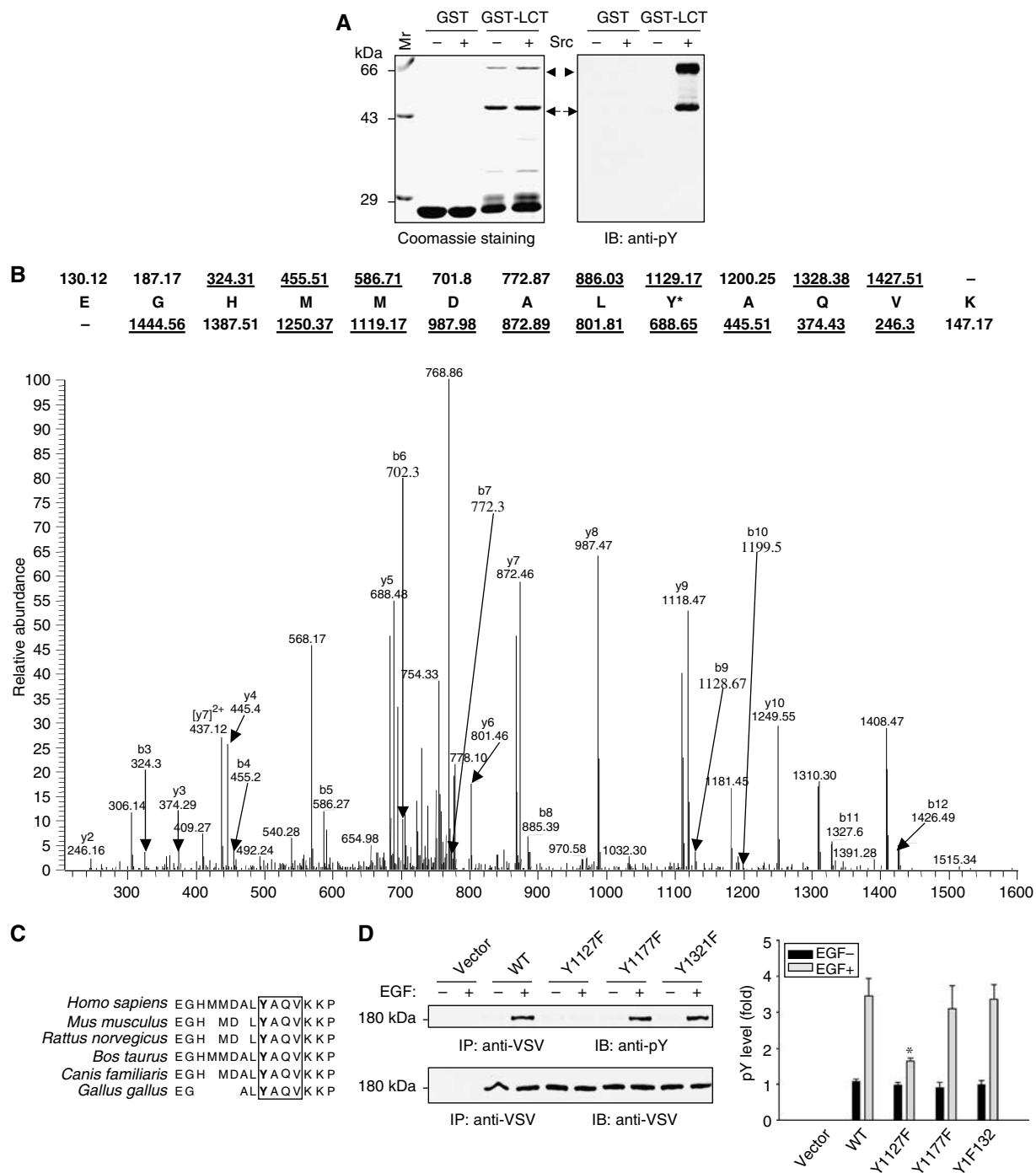


Figure 3 Identification of Par3 phosphotyrosine sites by *in vitro* and *in vivo* assays. (A) GST-Par3 LCT (1015–1356) and GST were phosphorylated or nonphosphorylated with c-Src in an *in vitro* kinase assay, electrophoresed with SDS-PAGE, and visualized by Coomassie staining (left panel) and immunoblotting with anti-pY (right panel). The arrowheads denote the GST fusion protein (left panel) or phosphotyrosine (right panel) signal of the fusion protein, whereas the arrows show the degraded GST-Par3 LCT. (B) The MS/MS spectra of the doubly charged form of the Y1127 phosphosite. The b- and y-ion series used for the phosphopeptide identification are indicated. Those observed are underlined. Y* represents the phosphotyrosine. (C) Sequence alignment of Par3 phosphotyrosine sites (Y1127) in different species. YAQV is the potential Csk (C-terminal Src kinase)-binding motif (rectangle). (D) MDCK cells were transfected with VSV-tagged plasmids of Par3, point mutation constructs, or the control vector, stimulated with or without EGF for 10 min, immunoprecipitated, and immunoblotted as indicated. The quantification of the immunoblot is shown on the right. Each value represents the mean \pm s.e.m. of three independent experiments. * $P < 0.05$ versus WT.

treated with PP2 before EGF stimulation, it progressed slowly, and reached a maximum of $2940 \pm 277 \Omega \text{cm}^2$ at 24 h, which was 60% of the TER from the cells treated with EGF alone ($P < 0.05$). In short, the inhibition of the SFKs activity impaired the ability of MDCK cells to form TJs in response to

EGF stimulation. Thus, activation of SFKs may be required for the EGF-induced TJ assembly.

To further emphasize the roles of the SFK members in EGF-promoted TJ formation, we analyzed MDCK cells transfected with the siRNAs for c-Src, c-Yes, or Fyn. The knockdown of

both c-Src and c-Yes caused a dramatic disruption of the TJ structure (Figure 4D and E), whereas the suppression of Fyn did not have an obvious effect (Figure 4D and E). In addition, the double knockdown of c-Src and c-Yes led to a profound negative effect on TJ formation (Figure 4D, panel 5 and E, columns 10 and 15). To complement the observations documenting the reductions in TJ formation by the knockdowns of c-Src and c-Yes, we examined the TER development in the cells exposed to EGF. As shown in Figure 4F, suppression of c-Src, or c-Yes, or both, but not Fyn, resulted in a marked attenuation of TER development, respectively. Collectively, the present data demonstrated that c-Src and c-Yes, but not Fyn, play important roles in EGF-induced TJ formation in MDCK cells.

Involvement of Par3 in EGF-promoted TJ formation

Previous studies using a calcium switch model demonstrated that Par3 is required for TJ formation in MDCK cells (Chen and Macara, 2005, 2006). However, it remains unclear whether Par3 is involved in EGF-controlled TJ assembly. To validate this point, siRNA of canine Par3 (cPar3) was transiently transfected into MDCK cells. As shown in Figure 5A, cPar3 siRNA suppressed the expression of endogenous Par3 approximately 80%, consistent with the published data by Chen and Macara (2005). Suppression of Par3 expression by Par3 siRNA led to a significant delay of TJ assembly induced by EGF treatment (Figure 5B and C). Furthermore, TER development in the Par3 knockdown cells was impaired significantly, as compared to that in the control cells ($P < 0.05$; Figure 5D). TER in the control cells peaked at $5190 \pm 60 \Omega \text{cm}^2$ at 12 h following the EGF treatment, whereas in the Par3 knockdown cells, TER in the peak showed a significantly low value of $3896 \pm 200 \Omega \text{cm}^2$ at a later time of 36 h after EGF stimulation. These data clearly implicate the involvement of Par3 in EGF-controlled formation of epithelial TJs.

Important role of Par3 phosphorylation at Y1127 residue in the TJ formation

To further investigate the biological significance of the identified phosphorylation sites of Par3, we generated several MDCK cell lines that stably expressed the VSV-tagged human wild-type Par3 (hPar3/WT), its three single tyrosine point mutants (hPar3/Y1127F, hPar3/Y1177F, and hPar3/Y1321F), and the control vector. Because the expression level of Par3 is crucial for TJ formation (Joberty *et al*, 2000), we confirmed that all selected transfectants demonstrated comparable expression levels of hPar3 and its mutants (Supplementary Figure S4). Overexpression of hPar3 and its mutants did not affect the expression of the TJ proteins ZO-1 and occludin (Supplementary Figure S4). To establish tyrosine phosphorylation of hPar3 and its mutants occurred in the transfectants, we precipitated the transfectants with anti-VSV antibody in the presence or absence of EGF. Western blot analysis of anti-pY revealed that mutation in Y1127, but not in the other tyrosine residues of hPar3, resulted in the abolishment of EGF-induced tyrosine phosphorylation of Par3 (Figure 6A), consistent with the previous results from the transient transfection experiments (Figure 3D). These results imply that EGF induces Par3 tyrosine phosphorylation exclusively at the Y1127 residue *in vivo*. To determine the role of Y1127 phosphorylation of hPar3 in TJ formation, we conducted immuno-

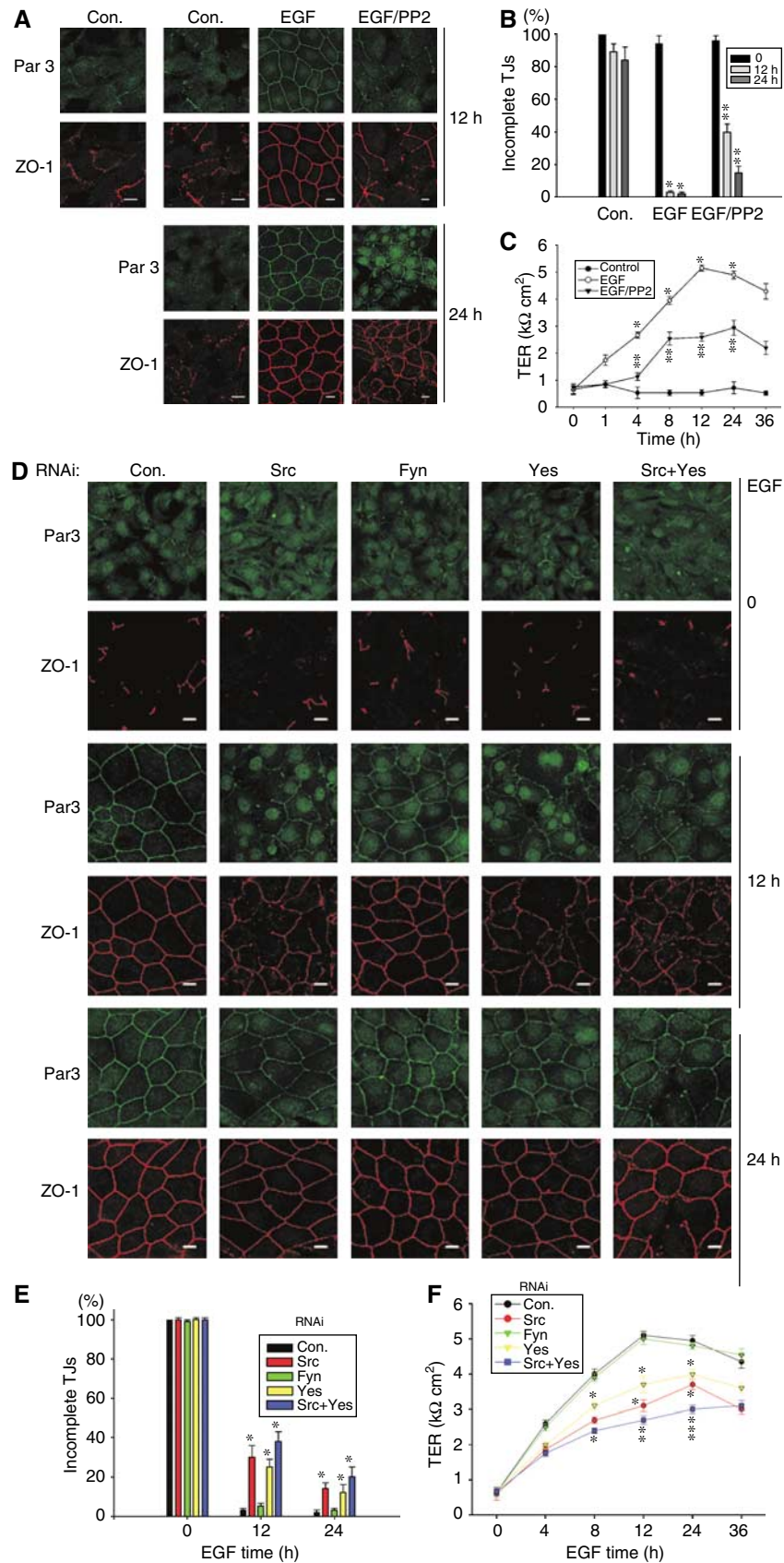
localization with anti-Par3 and ZO-1 antibodies in the transfectants (Figure 6B and C). According to our observation that MDCK cells complete their TJ structure formations after 12 h of EGF stimulation (Figure 4), an earlier time point (6 h) was chosen for further analysis. After 6 h of EGF treatment, approximately 70% of the cells stably overexpressing hPar3, hPar3/Y1177F, hPar3/1321F, or empty vector displayed similar abilities to form the complete TJ rings (Figure 6B and C). However, only about 40% of the cells expressing hPar3/Y1127F could complete the TJ ring formations (Figure 6B, middle panel and C, column 8). In addition, overexpression of wild-type hPar3 slightly increased TJ formation, as compared to the control cells (Figure 6C, column 7). After 24 h of EGF treatment, the TJ assemblages could completely ring at cell-cell contact expressing empty vector, wild type, Y1177F and Y1321F, whereas 15% of the hPar3/Y1127F-expressing cells did not complete the ZO-1 ring (Figure 6B, middle panel and C, column 13). In all cases, the transfectants without EGF stimulation were not able to form the TJ structure (Supplementary Figure S5).

To further establish the regulatory role of Par3 Y1127 phosphorylation on TJ formation, the development of TER was examined. As shown in Figure 6D, the TER of all of the cells remained constant, and fluctuated at approximately $500 \Omega \text{cm}^2$ in serum-free medium without EGF treatment (Figure 6D). However, the TER of the control cells peaked at $5100 \pm 160 \Omega \text{cm}^2$ after EGF-induction for 12 h, and then decreased, which was similar to normal MDCK cells (Figure 4C). The expression of hPar3 wild type, Y1177F, and Y1321F reproducibly promoted TER development in the early phase of EGF induction, as compared to that in the control cells (Figure 6D, asterisks). The TER values from those cells peaked to approximately $6000 \Omega \text{cm}^2$ after EGF induction for 8 h. In contrast, the expression of Y1127F decelerated the process of TJ assembly in the early stage significantly (Figure 6D; $P < 0.05$, double asterisks). To complement these electrophysiological observations, and to prove increased paracellular permeability by the expression of hPar3/Y1127F in MDCK monolayers, we examined the flux of a macromolecule across the epithelial monolayers of the selected EGF-exposed transfectants. Lucifer yellow was chosen as a marker of paracellular transport. The transport efficiency of lucifer yellow decreased following TJ formation (Irvine *et al*, 1999). The hPar3/Y1127F monolayers demonstrated significant enhancements in the paracellular flux of lucifer yellow, as compared to the other monolayers following 6 h of incubation with EGF (Figure 6E). However, after 24 h, the paracellular flux had decreased to similar levels in all cell lines. In short, overexpression of hPar3/Y1127F resulted in the delay of EGF-induced TJ formation in MDCK cells.

To further emphasize the role of hPar3 Y1127 in TJ formation, MDCK cells, of which endogenous Par3 was knocked down by cPar3 siRNA, were transfected with hPar3 or each of the three mutants. To investigate the rescue effect of different hPar3 plasmid, the specificity of cPar3 siRNA was confirmed, which was specific to canine-derived Par3 but not to human Par3 (Supplementary Figure S6). Supplementary Figure S7A shows the high efficiency of the endogenous cPar3 knockdown, and the expression of the transfected hPar3 and its mutants in MDCK cells. With these cells we conducted TER, lucifer yellow transport assays, and immunofluorescence following incubation with EGF at different time points

(Supplementary Figure S7B-E). As determined by the assays, the expression of hPar3/WT and its mutants, hPar3/Y1177F and hPar3/Y1321F, rescued the cPar3 siRNA-impaired TJ

formation (Supplementary Figure S7). The expression of hPar3/Y1127F could only partially recover the impaired TJ formation (Supplementary Figure S7). Taken together, phos-



phorylation of hPar3 at the Y1127 residue appears to be a key element in regulating EGF-promoted TJ assembly.

Phosphorylation of Par3 at Y1127 impairs the ability of Par3 to interact with LIMK2 and regulate cofilin phosphorylation

Next, we investigated the molecular mechanism of Y1127 phosphorylation in TJ assembly. Previous studies indicated that the C-terminus of Par3 contains several putative coiled-coil domains (Nishimura *et al*, 2004) that bind to Tiam1 (Chen and Macara, 2005; Nishimura *et al*, 2005) and/or LIM kinase 2 (Chen and Macara, 2006), thereby regulating TJ

formation. The motif analysis also revealed that the Y1127 residue in Par3 matches well with the Csk-binding motif (Figure 3C). We hypothesized that phosphorylation of Y1127 would alter or abolish the interaction ability of the Par3 C-terminus with its binding proteins, and impact the function of Par3 in epithelial TJ assembly. Indeed, following tyrosine phosphorylation of Par3 induced by EGF stimulation, the interaction of Par3/WT with LIMK2 was dramatically attenuated (down to 20%), while that of Par3/Y1127F was not affected (Figure 7A, top panel). However, Par3 tyrosine phosphorylation had no effect on its association with Tiam1 (Figure 7A, top second panel). In addition, we also found that

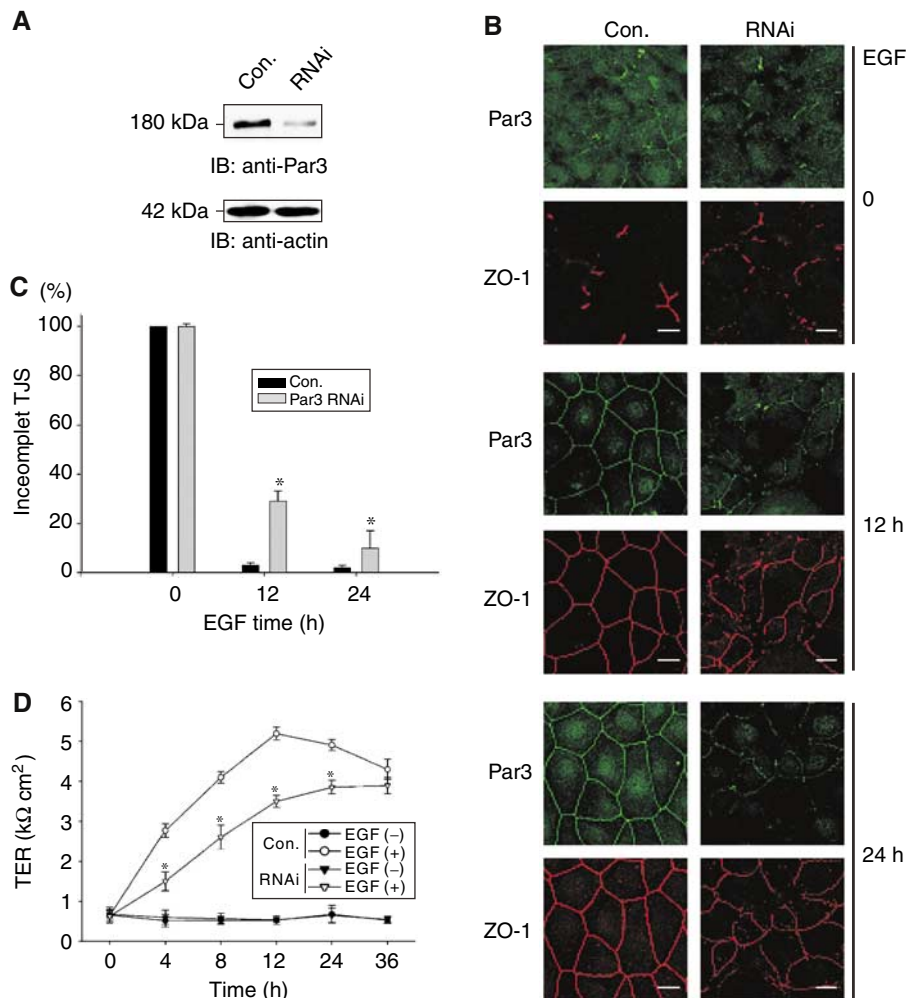


Figure 5 Par3 is necessary for EGF-induced TJ formation in MDCK cells. (A) The knockdown of endogenous Par3. MDCK cells were transiently transfected with either empty vector or the canine RNAi-targeting plasmid. Equal amounts of total proteins were analyzed with immunoblots. (B) Loss of Par3 significantly disrupts the localization of ZO-1 to cell borders. Scale bars: 10 μm. (C) Quantitative analysis of TJ assembly is shown, as indicated previously. **P*<0.05 versus control cells. (D) Loss of Par3 delays TER development. **P*<0.05 versus control cells.

Figure 4 c-Src and c-Yes are required for EGF-induced TJ assembly of MDCK cells. (A) Loss of SFK activity dramatically delays the TJ assembly during EGF stimulation. Scale bars: 10 μm. (B) Quantitative analysis of TJ assembly showing the percentage of cells that have incomplete peripheral ZO-1 staining. Each value represents the mean ± s.e.m. of three independent experiments. Student's *t*-test, **P*<0.05, EGF stimulation versus control cells; double asterisks (*P*<0.05) denote significant differences from the control or EGF-stimulated cells. (C) SFK inhibition delays the development of TER during EGF stimulation. The kinetics of TER development in MDCK cells was tracked for 36 h after the addition of EGF. Each value represents the mean ± s.e.m. of three independent experiments. Student's *t*-test, **P*<0.05, EGF stimulation versus control cells and double asterisks (*P*<0.05) denote significant differences from the control or EGF-stimulated cells. (D) The knockdown of c-Src and c-Yes delays TJ assembly. Scale bars: 10 μm. (E) Quantitative analysis of TJ assembly was shown just as indicated in (B). **P*<0.05 versus control cells. (F) The knockdown of c-Src and c-Yes delays the development of TER in MDCK cells. **P*<0.05 versus control cells, ***P*<0.05 versus c-Yes knockdown cells, ****P*<0.05 versus both c-Src and c-Yes knockdown cells.

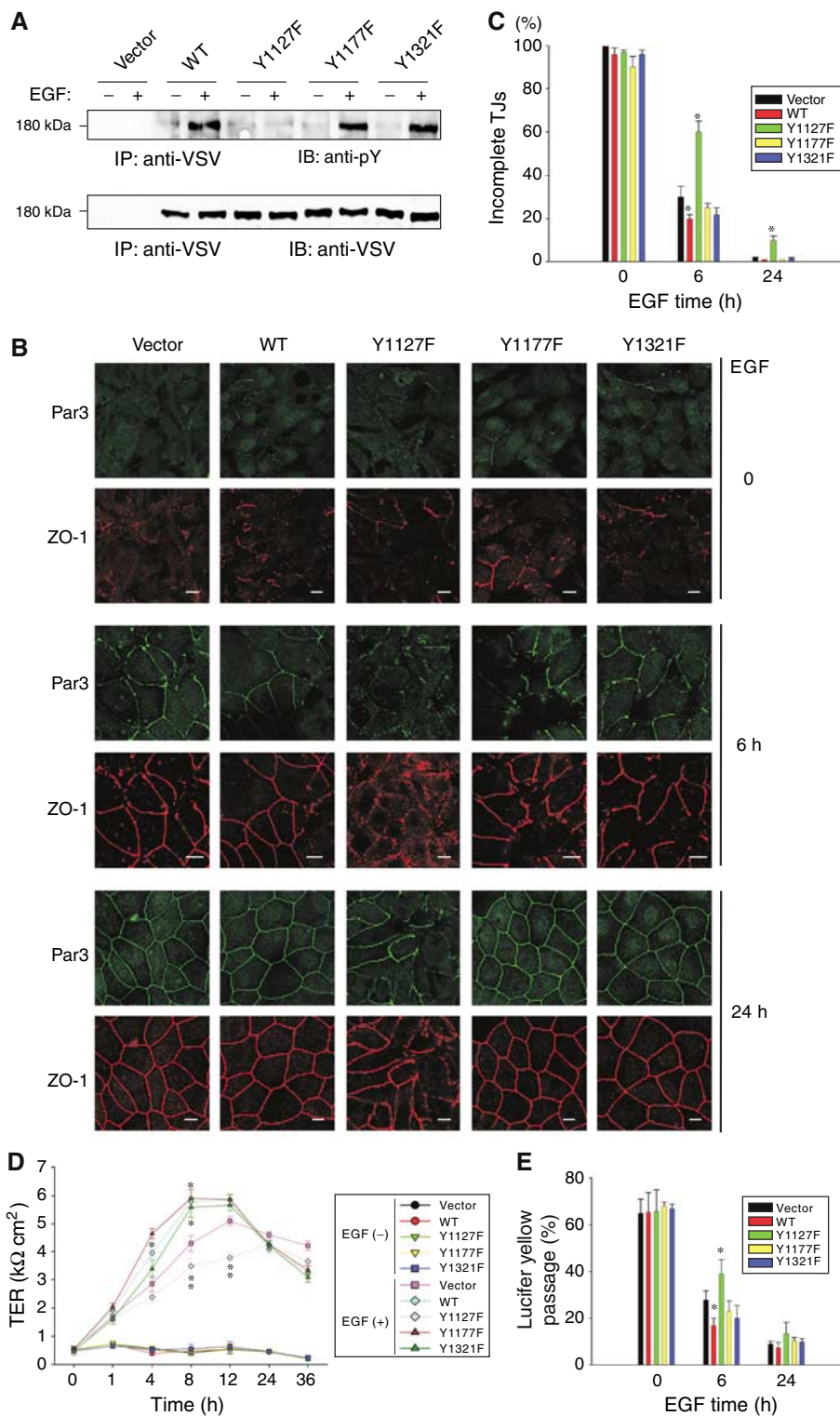


Figure 6 Tyrosine phosphorylation of Par3 promotes EGF-induced TJ formation in MDCK cells. **(A)** Y1127 is the major phosphotyrosine site of Par3 responsible for EGF stimulation in MDCK stable cells. MDCK stable cells were stimulated or nonstimulated with or without EGF, respectively, for 10 min, immunoprecipitated and immunoblotted as indicated. **(B)** Par3 Y1127F delays TJ assembly in MDCK cells. Scale bars: 10 μ m. **(C)** Quantitative analysis of TJ assembly showing the percentage of cells that has incomplete peripheral ZO-1 staining. Each value represents the mean \pm s.e.m. of three independent experiments. Student's *t*-test, **P* < 0.05, difference from control (vector) cells. **(D)** Par3 Y1127F delays the development of TER during EGF stimulation. Student's *t*-test, **P* < 0.05, significant difference from control (vector) cells; ***P* < 0.05, significant difference from control (vector) and other cells. **(E)** Paracellular passage of lucifer yellow across MDCK cell monolayers was measured at 0, 6, and 24 h after EGF stimulation. Student's *t*-test, **P* < 0.05, significant difference from control (vector) cells.

the tyrosine phosphorylated Par3/WT, but not its mutant Par3/Y1127F, was able to recruit Csk in an EGF-stimulated manner (Figure 7A, middle panel).

More recently, an investigation by Chen and Macara (2006) indicated that Par3 mediated the inhibition of LIMK2 activity via protein–protein interaction, thereby regulating cofilin

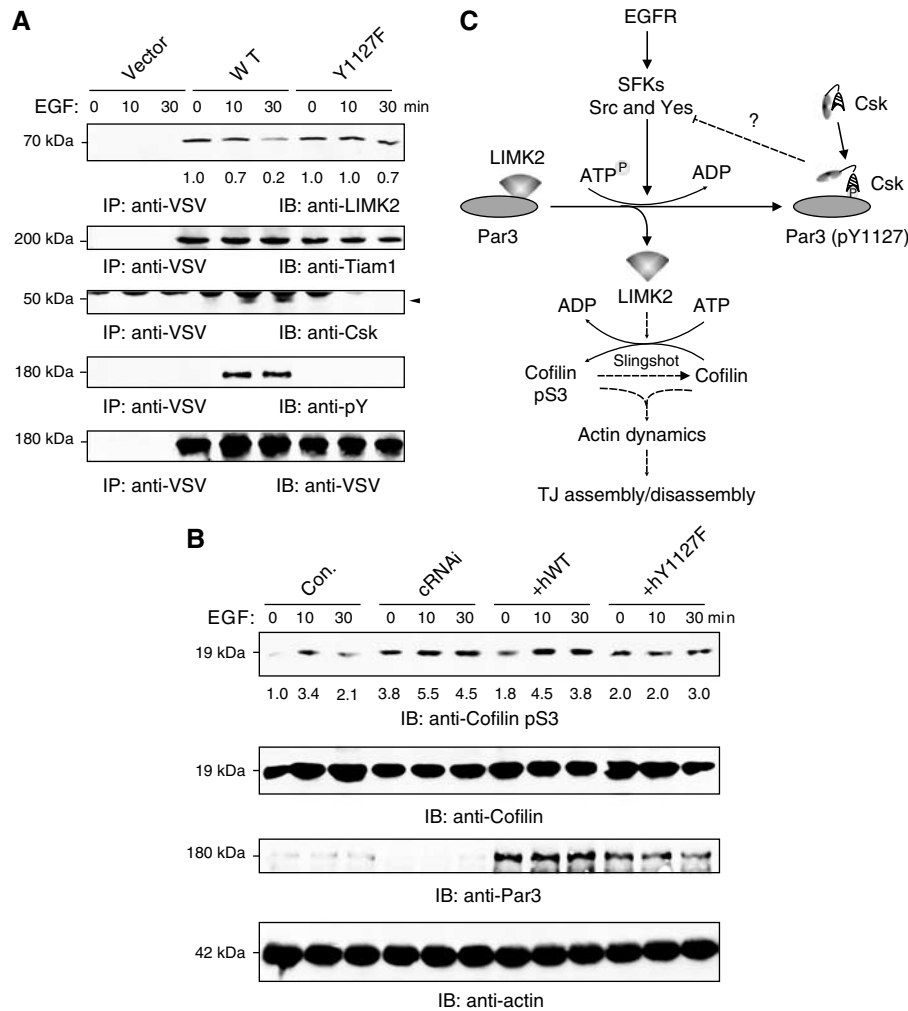


Figure 7 Phosphotyrosine site of Par3 regulates its association with LIMK2 and Csk. **(A)** MDCK cells were transfected with VSV-tagged Par3/WT, Par3/Y1127F, or control vector, and stimulated with or without EGF for 10 min, immunoprecipitated and immunoblotted as indicated. The relative level of associated LIMK2 is shown. The arrowhead shows the position of Csk near the IgG heavy chain. **(B)** Par3 Y1127F destroyed the dynamics of phospho-cofilin induced by EGF. The total cell lysates from cells with the knockdown of canine-sourced Par3 (cPar3) or the re-addition of different human-sourced Par3 (hPar3) plasmids were analyzed by immunoblotting procedures. The relative phosphorylation level of cofilin is shown. **(C)** EGFR-mediated signaling pathway in TJ formation. The tyrosine-phosphorylated Par3 by EGFR-SFKs signaling negatively regulates the Par3-LIMK2 interaction, and results in the recruitment of Csk. The free LIMK2 phosphorylates its substrate cofilin at Serine 3. On the other hand, the phospho-cofilin can be dephosphorylated by Slingshot. EGF-induced Par3-Csk interaction may inhibit the activity of the SFKs. The lines indicate the works in this study. The dashed indicate the published data.

phosphorylation dynamics and TJ assembly. Thus, we explored whether phosphorylated Par3 could influence cofilin phosphorylation in response to EGF stimulation. As shown in Figure 7B, EGF stimulation induced cofilin phosphorylation, consistent with previous findings by Mouneimne *et al* (2004). A Par3 knockdown enhanced the phosphorylation of cofilin compared to control cells in the absence of EGF, which is also consistent with the findings by Chen and Macara (2006). Upon EGF stimulation, cofilin phosphorylation in the Par3 knockdown cells was further increased and maintained consistently at the high level (Figure 7B). In the absence of EGF, re-transfection with either hPar3/WT or hPar3/Y1127F to the Par3-knockdown cells could partially reverse cofilin phosphorylation, as compared to that in the Par3-knockdown cells (Figure 7B). In the presence of EGF, re-transfection with hPar3/WT appeared to have little effect on cofilin phosphorylation. Interestingly, EGF stimulation had no more effect on cofilin phosphorylation in the cells re-transfected with hPar3/

Y1127F (Figure 7B), indicating that phosphorylation of Y1127 controlled by EGF signaling may play a critical role in the phosphorylation dynamics of cofilin. In conclusion, we propose that EGF-induced phosphorylation of Par3 reduces its association with LIMK2, thereby enabling LIMK2 to regulate the phosphorylation dynamics of cofilin and TJ assembly.

Discussion

Phosphorylation is a basic and important regulatory means of signal transduction. Herein, we profiled phosphotyrosine proteins induced by pervanadate treatment utilizing a phospho-proteomic approach. In our identified profiling schema, several cell polarity proteins were found, such as Par3, WARTS (LATS1), and hFat2, indicating that tyrosine phosphorylation may be an essential element for cell polarity regulation (Verde *et al*, 1998; Macara, 2004; Matakatsu and Blair, 2004). Phosphorylation and its function in Par3-

mediated TJ formation have been explored previously. For example, serine 144 phosphorylation of Par3 is vital for cell polarity formation in epithelial cells, as point mutation of S144 to alanine resulted in cell polarity defects (Hurd *et al*, 2003a). Another serine residue phosphorylated by aPKC (S827) is crucial for Par3 location and TJ formation (Hirose *et al*, 2002). Recently, proteomic analysis has revealed three novel Par3 phosphorylation sites at tyrosines 388, 1080, and 1177 (Supplementary Figure S8), whereas in the present study, we found that all Par3 isoforms incurred phosphorylation events upon treatment of POV in HEK293 cells (data not shown), indicating that Par3 may contain multiple tyrosine phosphorylation sites. Indeed, our data indicated that Par3 Y1127, Y1177, and Y1321 can all be phosphorylated (Figure 3 and Supplementary Figure S3).

Owing to the vital role of Par3 in establishing and maintaining cell polarity and TJ assembly, it is important to define the upstream signaling members that target tyrosine residues of Par3. Our data clearly demonstrated that EGFR signaling selectively evokes phosphorylation of Par3 180K, but not the other forms (Figure 1). Further, the point mutation analysis demonstrated that Par3 Y1127 is the major phosphorylation site targeted by EGF-induced signaling *in vivo*. The functional importance of Par3 Y1127 in EGF-promoted TJ formation was demonstrated by the TER and paracellular transport assays, as well as the knockdown rescue assay (Figure 6 and Supplementary Figure S7). Par3/WT and its two mutants, Y1177F and Y1321F, were able to rescue the Par3 knockdown phenotype completely, whereas Par3/Y1127F only partially rescues the Par3 knockdown phenotype, indicating that tyrosine phosphorylation of Par3 may not be essential, but is required for optimum epithelial TJ assembly by EGF. Currently, it is unclear which cell signaling events target the other phosphorylation sites of Par3 apart from Y1127. Coexpression of RTKs with Par3 in HEK293 cells (Figure 1A) indicates that Par3 may be involved in multiple RTK-signaling pathways. The other phosphotyrosine sites may also be the potential secondary nonpreferential substrates for SFKs *in vivo*, or are likely targeted by other tyrosine kinases.

The SFK family was thought to be required for epithelial TJ dynamics (Yap *et al*, 1997; Tsukamoto and Nigam, 1999; Meyer *et al*, 2001; Chen *et al*, 2002). The bidirectional interaction of EGFR and SFKs generates a synergistic cellular signaling event for promoting a variety of cell actions, as well as cell transformation in pathological conditions (Ishizawa and Parsons, 2004). However, it was unclear whether SFK plays a role in EGF-induced TJ formation. This issue is resolved herein with pharmaceutical interference and RNA interference approaches (Figure 4). Our data demonstrated that c-Src and c-Yes are required for EGF-induced Par3 tyrosine phosphorylation *in vivo* (Figure 4). Thus, once bound by the ligand, EGFR molecules dimerize, autophosphorylate, and recruit the SFKs. The association of EGFR and SFKs results in the activation of SFKs. Meanwhile, SFK is likely to phosphorylate its downstream targets, such as Par3, possibly also occludin and ZO-1 (Yap *et al*, 1997; Tsukamoto and Nigam, 1999; Chen *et al*, 2002), which may modify TJ protein activity thereby regulating TJ formation.

It is also well known that the SFKs, EGFR and its family members, including HER2, are overexpressed in many of the same tumor types, and participate in regulating cell transfor-

mation and tumorigenesis. Loss of cell polarity is a landmark event in cancer cells and carcinoma progression during the invasive and metastatic phases (Humbert *et al*, 2003). Abnormal compartmentalization of membrane receptors in cells with impaired TJ may result in dysfunction of cellular signaling, which in turn leads to cell transformation and tumorigenesis (Amsler and Kuwada, 1999; Vermeer *et al*, 2003, 2006). In tumor cells, dysfunction of growth factor receptors may conduce to aberrant tyrosine phosphorylation of Par3, leading to pathological TJ assembly and disassembly. Overexpression of c-Src kinase in 293T cells, indeed, induced tyrosine phosphorylation of all three forms of Par3 (data not shown). Multiple tyrosine phosphorylation sites of Par3 were also reported through proteome screening (Supplementary Figure S8). Therefore, it will be very interesting to determine whether overactivated EGFR-SFK signaling, or the loss of defined signaling molecules, could lead hyperphosphorylation of Par3 at multiple tyrosine residues, and whether this is involved in tumorigenesis under pathological conditions.

Tyrosine-phosphorylated TJ proteins such as ZO-1 and occludin are well known to be involved in TJ dynamics. However, the molecular mechanism of tyrosine phosphorylation in epithelial TJ assembly and cell polarity remains poorly understood. The data presented herein clearly demonstrated for the first time that EGF signaling regulates Par3 tyrosine phosphorylation at Y1127 and subsequently negatively tunes the interaction between Par3 and LIMK2 (Figure 7A), which in turn regulates cofilin phosphorylation (Figure 7B), actin dynamics (data not shown), and TJ assembly. On the other hand, a point mutation of Par3, Y1127F, abolished the EGF-induced impairment of the Par3-LIMK2 interaction (Figure 7A), negating the effect of EGF on cofilin phosphorylation (Figure 7B). As LIMK2 directly binds to the C-terminus of Par3, it is likely that phosphorylation of Par3 Y1127 leads to spatial occupation and/or altered conformation of the Par3 C-terminus, thereby reducing the interaction between Par3 and LIMK2 (Figure 7C). In addition, our results also suggested another important function of phosphorylated Par3 Y1127, namely recruiting Csk, a key negative regulatory kinase for SFKs (Chong *et al*, 2005). Thus, phosphorylated Par3 might mediate a negative feedback loop, consisting of Par3, Csk, and SFKs (Figure 7C). It would be interesting to further examine whether this potential feedback loop balances the regulatory activity of SFK on the interaction of Par3 and LIMK2 to influence actin dynamics. Altogether, our current study suggests a possible role of Par3 tyrosine phosphorylation induced by EGF signaling in modulating actin dynamics to promote epithelial TJ assembly and polarization.

Materials and methods

Materials

The monoclonal antibodies (mAbs) anti-phosphotyrosine (4G10) and c-Src were purchased from Upstate. The mAb anti-V5 tag was purchased from ADI. The mAbs anti-ZO-1 and occludin were purchased from Zymed. The mAb anti-actin was purchased from Sigma. The mAbs anti-c-Yes and Fyn were purchased from BD Pharmingen. The polyclonal antibodies (pAbs) anti-pcofilin, cofilin, and LIMK2 were purchased from Cell Signaling Technology. The pAb anti-Tiam1 was purchased from Santa Cruz. We generated the polyclonal Par3 antibodies against the Par3 PDZ 2-3 domain (425-695aa) or C-terminus (LCT; 1111-1353aa) of the GST fusion construct. These antibodies were affinity-purified by passing the serum sequentially over CNBr-linked GST and the corresponding

GST-tagged PDZ 2-3 or Par3 LCT sepharose columns (Amersham Pharmacia). Secondary antibodies for the immunoblot and immunofluorescence assays were purchased from Sigma and Molecular Probes, respectively. The human sourced Par3 180K plasmid and the RNAi plasmid of canine Par3 were kindly provided by Dr Ian G Macara (University of Virginia, USA) and Xinyu Chen (University of Virginia, USA), respectively. The three isoforms of Par3 (100K, 150K, and 180K) were subcloned into pcDNA3-VSV vectors. The point mutants of Par3 were introduced by point mutagenesis procedures according to the manufacturer's instructions (Stratagene). All of the RNAi target sequences in this study are listed in Supplementary Table S2. The construction of the plasmids containing the growth factor receptors and pAb anti-Csk were described previously (Kharitonov *et al*, 1997; Jiang *et al*, 2006).

Cell culture, transfection, and immunofluorescence

The 293T and MDCK cells were cultured in Dulbecco's modified Eagle's medium (DMEM) supplemented with 10% calf serum at 37°C and 5% CO₂. The cells were transiently transfected using lipofectamineTM 2000 (Invitrogen). For the gene knockdown and rescue assay, MDCK cells (1×10^7) were electroporated with 20 µg plasmid using Gene Pulser XcellTM Electroporation System (Bio-Rad). For the immunofluorescence experiments, to avoid the influence of EGF stimulation on cell proliferation, MDCK cell monolayers were first grown to 100% confluence in DMEM complete medium and then the medium was replaced with serum-free media. After 15 h, the cells were either untreated or stimulated with EGF (100 ng/ml) for appropriate time. If PP2 was used, 10 µM PP2 were first added to the medium for 30 min before EGF stimulation. The immunofluorescence was carried out according to previous description (Wang *et al*, 2006). To quantify the effects on TJ assembly, ZO-1 staining between cells was counted as either 'complete' or 'incomplete'. For each condition, three groups

of 100 cell-cell contacts were counted from three independent experiments. Statistical analysis was performed using two-tailed Student's *t*-test.

Immunoprecipitation and immunoblot

The samples were immunoprecipitated and immunoblotted with appropriate antibodies just as described previously (Wang *et al*, 2006). The protein patterns were recorded as digitalized images using a high-resolution scanner (GS-800, Bio-Rad). Gel images were analyzed with QuantityOne software (Bio-Rad).

TER and lucifer yellow passage assay

The TER assay and lucifer yellow assay were conducted using the methods described previously (Irvine *et al*, 1999; Singh and Harris, 2004). The detailed procedures were shown in Supplementary Section.

Supplementary data

Supplementary data are available at *The EMBO Journal* Online (<http://www.embojournal.org>).

Acknowledgements

We thank Dr Yingjie Wu and Dr Dangsheng Li for critical reading of the manuscript, Dr Ian G Macara, Dr Xingyu Chen, and Dr T Nakamura for hPar3, cPar3 RNAi, and rat LIMK2 plasmids, respectively. We appreciated Rongxia Li and Hu Zhou for MS help, and Jinbo Han for helpful discussion. This research was supported by grants from Ministry of Science and Technology (2002BA711A11 and 2001CB510205) and the National Natural Science Foundation of China (30170208).

References

- Amsler K, Kuwada SK (1999) Membrane receptor location defines receptor interaction with signaling proteins in a polarized epithelium. *Am J Physiol* **276**: C91–C101
- Basuroy S, Seth A, Elias B, Naren AP, Rao R (2006) MAPK interacts with occludin and mediates EGF-induced prevention of tight junction disruption by hydrogen peroxide. *Biochem J* **393**: 69–77
- Bromann PA, Korkaya H, Courtneidge SA (2004) The interplay between Src family kinases and receptor tyrosine kinases. *Oncogene* **23**: 7957–7968
- Chen X, Macara IG (2005) Par-3 controls tight junction assembly through the Rac exchange factor Tiam1. *Nat Cell Biol* **7**: 262–269
- Chen X, Macara IG (2006) Par-3 mediates the inhibition of LIM kinase 2 to regulate cofilin phosphorylation and tight junction assembly. *J Cell Biol* **172**: 671–678
- Chen YH, Lu Q, Goodenough DA, Jeansson B (2002) Nonreceptor tyrosine kinase c-Yes interacts with occludin during tight junction formation in canine kidney epithelial cells. *Mol Biol Cell* **13**: 1227–1237
- Chong YP, Mulhern TD, Cheng HC (2005) C-terminal Src kinase (CSK) and CSK-homologous kinase (CHK)—endogenous negative regulators of Src-family protein kinases. *Growth Factors* **23**: 233–244
- Gonzalez-Mariscal L, Betanzos A, Nava P, Jaramillo BE (2003) Tight junction proteins. *Prog Biophys Mol Biol* **81**: 1–44
- Harhaj NS, Barber AJ, Antonetti DA (2002) Platelet-derived growth factor mediates tight junction redistribution and increases permeability in MDCK cells. *J Cell Physiol* **193**: 349–364
- Hirose T, Izumi Y, Nagashima Y, Tamai-Nagai Y, Kurihara H, Sakai T, Suzuki Y, Yamanaka T, Suzuki A, Mizuno K, Ohno S (2002) Involvement of ASIP/PAR-3 in the promotion of epithelial tight junction formation. *J Cell Sci* **115**: 2485–2495
- Humbert P, Russell S, Richardson H (2003) Dlg, Scribble and Lgl in cell polarity, cell proliferation and cancer. *BioEssays* **25**: 542–553
- Hurd TW, Fan S, Liu CJ, Kweon HK, Hakansson K, Margolis B (2003a) Phosphorylation-dependent binding of 14-3-3 to the polarity protein Par3 regulates cell polarity in mammalian epithelia. *Curr Biol* **13**: 2082–2090
- Hurd TW, Gao L, Roh MH, Macara IG, Margolis B (2003b) Direct interaction of two polarity complexes implicated in epithelial tight junction assembly. *Nat Cell Biol* **5**: 137–142
- Irvine JD, Takahashi L, Lockhart K, Cheong J, Tolan JW, Selick HE, Grove JR (1999) MDCK (Madin–Darby canine kidney) cells: a tool for membrane permeability screening. *J Pharm Sci* **88**: 28–33
- Ishizawa R, Parsons SJ (2004) c-Src and cooperating partners in human cancer. *Cancer Cell* **6**: 209–214
- Jiang LQ, Feng X, Zhou W, Knyazev PG, Ullrich A, Chen Z (2006) Csk-binding protein (Cbp) negatively regulates epidermal growth factor-induced cell transformation by controlling Src activation. *Oncogene* **25**: 5495–5506
- Joberty G, Petersen C, Gao L, Macara IG (2000) The cell-polarity protein Par6 links Par3 and atypical protein kinase C to Cdc42. *Nat Cell Biol* **2**: 531–539
- Kharitonov A, Chen Z, Sures I, Wang H, Schilling J, Ullrich A (1997) A family of proteins that inhibit signalling through tyrosine kinase receptors. *Nature* **386**: 181–186
- Lin D, Edwards AS, Fawcett JP, Mbamalu G, Scott JD, Pawson T (2000) A mammalian PAR-3–PAR-6 complex implicated in Cdc42/Rac1 and aPKC signalling and cell polarity. *Nat Cell Biol* **2**: 540–547
- Macara IG (2004) Parsing the polarity code. *Nat Rev Mol Cell Biol* **5**: 220–231
- Matakatsu H, Blair SS (2004) Interactions between fat and Dachsous and the regulation of planar cell polarity in the *Drosophila* wing. *Development* **131**: 3785–3794
- Matter K, Aijaz S, Tsapara A, Balda MS (2005) Mammalian tight junctions in the regulation of epithelial differentiation and proliferation. *Curr Opin Cell Biol* **17**: 453–458
- Matter K, Balda MS (2003) Signalling to and from tight junctions. *Nat Rev Mol Cell Biol* **4**: 225–236
- Meyer TN, Schwesinger C, Ye J, Denker BM, Nigam SK (2001) Reassembly of the tight junction after oxidative stress depends on tyrosine kinase activity. *J Biol Chem* **276**: 22048–22055
- Mouneimne G, Soon L, DesMarais V, Sidani M, Song X, Yip SC, Ghosh M, Eddy R, Backer JM, Condeelis J (2004) Phospholipase C and cofilin are required for carcinoma cell directionality in response to EGF stimulation. *J Cell Biol* **166**: 697–708

- Nishimura T, Kato K, Yamaguchi T, Fukata Y, Ohno S, Kaibuchi K (2004) Role of the PAR-3-KIF3 complex in the establishment of neuronal polarity. *Nat Cell Biol* **6**: 328–334
- Nishimura T, Yamaguchi T, Kato K, Yoshizawa M, Nabeshima Y, Ohno S, Hoshino M, Kaibuchi K (2005) PAR-6-PAR-3 mediates Cdc42-induced Rac activation through the Rac GEFs STEF/Tiam1. *Nat Cell Biol* **7**: 270–277
- Nunbhakdi-Craig V, Machleidt T, Ogris E, Bellotto D, White III CL, Sontag E (2002) Protein phosphatase 2A associates with and regulates atypical PKC and the epithelial tight junction complex. *J Cell Biol* **158**: 967–978
- Ohno S (2001) Intercellular junctions and cellular polarity: the PAR-aPKC complex, a conserved core cassette playing fundamental roles in cell polarity. *Curr Opin Cell Biol* **13**: 641–648
- Ozdamar B, Bose R, Barrios-Rodiles M, Wang HR, Zhang Y, Wrana JL (2005) Regulation of the polarity protein Par6 by TGFbeta receptors controls epithelial cell plasticity. *Science* **307**: 1603–1609
- Park J, Cartwright CA (1995) Src activity increases and Yes activity decreases during mitosis of human colon carcinoma cells. *Mol Cell Biol* **15**: 2374–2382
- Plant PJ, Fawcett JP, Lin DC, Holdorf AD, Binns K, Kulkarni S, Pawson T (2003) A polarity complex of mPar-6 and atypical PKC binds, phosphorylates and regulates mammalian Lgl. *Nat Cell Biol* **5**: 301–308
- Pollack AL, Apodaca G, Mostov KE (2004) Hepatocyte growth factor induces MDCK cell morphogenesis without causing loss of tight junction functional integrity. *Am J Physiol Cell Physiol* **286**: C482–C494
- Sargiacomo M, Sudol M, Tang Z, Lisanti MP (1993) Signal transducing molecules and glycosyl-phosphatidylinositol-linked proteins form a caveolin-rich insoluble complex in MDCK cells. *J Cell Biol* **122**: 789–807
- Sawada N, Murata M, Kikuchi K, Osanai M, Tobioka H, Kojima T, Chiba H (2003) Tight junctions and human diseases. *Med Electron Microsc* **36**: 147–156
- Schwabe T, Bainton RJ, Fetter RD, Heberlein U, Gaul U (2005) GPCR signaling is required for blood-brain barrier formation in *Drosophila*. *Cell* **123**: 133–144
- Singh AB, Harris RC (2004) Epidermal growth factor receptor activation differentially regulates claudin expression and enhances transepithelial resistance in Madin-Darby canine kidney cells. *J Biol Chem* **279**: 3543–3552
- Songyang Z, Shoelson SE, McGlade J, Olivier P, Pawson T, Bustelo XR, Barbacid M, Sabe H, Hanafusa H, Yi T, Ren R, Baltimore D, Ratnofsky S, Feldman RA, Cantley LC (1994) Specific motifs recognized by the SH2 domains of Csk, 3BP2, fps/fes, GRB-2, HCP, SHC, Syk, and Vav. *Mol Cell Biol* **14**: 2777–2785
- Spicer J, Ashworth A (2004) LKB1 kinase: master and commander of metabolism and polarity. *Curr Biol* **14**: R383–R385
- Tsukamoto T, Nigam SK (1999) Role of tyrosine phosphorylation in the reassembly of occludin and other tight junction proteins. *Am J Physiol* **276**: F737–F750
- Van Itallie CM, Balda MS, Anderson JM (1995) Epidermal growth factor induces tyrosine phosphorylation and reorganization of the tight junction protein ZO-1 in A431 cells. *J Cell Sci* **108** (Part 4): 1735–1742
- Verde F, Wiley DJ, Nurse P (1998) Fission yeast orb6, a ser/thr protein kinase related to mammalian rho kinase and myotonic dystrophy kinase, is required for maintenance of cell polarity and coordinates cell morphogenesis with the cell cycle. *Proc Natl Acad Sci USA* **95**: 7526–7531
- Vermeer PD, Einwalter LA, Moninger TO, Rokhlina T, Kern JA, Zabner J, Welsh MJ (2003) Segregation of receptor and ligand regulates activation of epithelial growth factor receptor. *Nature* **422**: 322–326
- Vermeer PD, Panko L, Welsh MJ, Zabner J (2006) erbB1 functions as a sensor of airway epithelial integrity by regulation of protein phosphatase 2A activity. *J Biol Chem* **281**: 1725–1730
- Vinot S, Le T, Ohno S, Pawson T, Maro B, Louvet-Vallee S (2005) Asymmetric distribution of PAR proteins in the mouse embryo begins at the 8-cell stage during compaction. *Dev Biol* **282**: 307–319
- Wang Y, Li R, Du D, Zhang C, Yuan H, Zeng R, Chen Z (2006) Proteomic analysis reveals novel molecules involved in insulin signaling pathway. *J Proteome Res* **5**: 846–855
- Yap AS, Stevenson BR, Cooper V, Manley SW (1997) Protein tyrosine phosphorylation influences adhesive junction assembly and follicular organization of cultured thyroid epithelial cells. *Endocrinology* **138**: 2315–2324
- Yoshida K, Kanaoka S, Takai T, Uezato T, Miura N, Kajimura M, Hishida A (2005) EGF rapidly translocates tight junction proteins from the cytoplasm to the cell-cell contact via protein kinase C activation in TMK-1 gastric cancer cells. *Exp Cell Res* **309**: 397–409